

This article was downloaded by:

On: 26 January 2011

Access details: *Access Details: Free Access*

Publisher *Taylor & Francis*

Informa Ltd Registered in England and Wales Registered Number: 1072954 Registered office: Mortimer House, 37-41 Mortimer Street, London W1T 3JH, UK



## Nucleosides, Nucleotides and Nucleic Acids

Publication details, including instructions for authors and subscription information:

<http://www.informaworld.com/smpp/title~content=t713597286>

### Physico-chemical and Biological Properties of Antisense Phosphodiester Oligonucleotides with Various Secondary Structures

Andrei V. Maksimenko<sup>a</sup>; Marina B. Gottikh<sup>a</sup>; Valerie Helin<sup>b</sup>; Zoe A. Shabarova<sup>a</sup>; Claude Malvy<sup>b</sup>

<sup>a</sup> Belozersky Institute of Physical Chemical Biology and Chemical Department, Lomonosov Moscow State University, Moscow, Russia <sup>b</sup> Laboratoire de Biochimie-Enzymologie, Institut Gustave Roussy, Villejuif, France

**To cite this Article** Maksimenko, Andrei V. , Gottikh, Marina B. , Helin, Valerie , Shabarova, Zoe A. and Malvy, Claude(1999) 'Physico-chemical and Biological Properties of Antisense Phosphodiester Oligonucleotides with Various Secondary Structures', *Nucleosides, Nucleotides and Nucleic Acids*, 18: 9, 2071 — 2091

**To link to this Article:** DOI: 10.1080/07328319908044865

**URL:** <http://dx.doi.org/10.1080/07328319908044865>

PLEASE SCROLL DOWN FOR ARTICLE

Full terms and conditions of use: <http://www.informaworld.com/terms-and-conditions-of-access.pdf>

This article may be used for research, teaching and private study purposes. Any substantial or systematic reproduction, re-distribution, re-selling, loan or sub-licensing, systematic supply or distribution in any form to anyone is expressly forbidden.

The publisher does not give any warranty express or implied or make any representation that the contents will be complete or accurate or up to date. The accuracy of any instructions, formulae and drug doses should be independently verified with primary sources. The publisher shall not be liable for any loss, actions, claims, proceedings, demand or costs or damages whatsoever or howsoever caused arising directly or indirectly in connection with or arising out of the use of this material.

## PHYSICO-CHEMICAL AND BIOLOGICAL PROPERTIES OF ANTISENSE PHOSPHODIESTER OLIGONUCLEOTIDES WITH VARIOUS SECONDARY STRUCTURES

Andrei V. Maksimenko<sup>1,2</sup>, Marina B. Gottikh<sup>1\*</sup>, Valerie Helin<sup>2</sup>,  
Zoe A. Shabarova<sup>1</sup> and Claude Malvy<sup>2</sup>

<sup>1</sup>Belozersky Institute of Physical Chemical Biology and Chemical Department,  
Lomonosov Moscow State University, 119899 Moscow, Russia;

<sup>2</sup>Laboratoire de Biochimie-Enzymologie, UMR CNRS 1772, Institut Gustave Roussy,  
94805 Villejuif, France.

**ABSTRACT:** The influence of the secondary structure of oligonucleotides having a natural phosphodiester backbone on their ability to interact with DNA and RNA targets and on their resistance to the nucleolytic digestion is investigated. Oligonucleotides having hairpin, looped and snail-like structure are found to be much more stable to nuclease degradation in different biological media and inside cells than the linear ones. The structured oligonucleotides can also hybridise with their DNA and RNA targets.

### INTRODUCTION

Regulation of gene expression by antisense oligonucleotides (ODNs) has provided a powerful approach for the study of gene function and inhibition of genes responsible for undesirable traits (1-3). One of the major problems encountered in using phosphodiester ODNs is their rapid degradation by various nucleases in cell cultures (4, 5). Modifications of the phosphodiester backbone have been used to enhance ODN stability against the enzymatic hydrolysis (6-8). However, these modifications are often accompanied by the loss of other properties important for the antisense activity (affinity for RNA targets, ability to mediate the RNase H degradation of targeted RNAs) (1, 7, 9). Moreover, modified ODNs can often acquire undesirable properties such as non-specific interaction with cellular proteins and cytotoxicity (10-14).

In order to stabilise antisense phosphodiester ODNs against nuclease degradation, some efforts including a synthesis of ODNs with a special secondary structure have been made. ODNs having a thermostable 3'-terminal mini-hairpin fragment are shown to be much more resistant to the 3'-exonuclease hydrolysis (15-17). The increased exonuclease resistance of such ODNs results in their improved antisense activity, in particular, against herpes simplex virus proliferation in cells (16). Evidently, 5'-end hairpins can protect ODNs against 5'-exonuclease degradation. However, terminal mini-hairpins are unable to protect ODNs against endonucleases. To minimise a risk of the ODN endonuclease degradation, antisense ODNs having an extended double stranded domain and a short single stranded part which is the most sensitive to endonucleases seem to be very promising. The single stranded part must provide the recognition of a complementary sequence in a targeted nucleic acid. The intramolecular ODN duplex has to be stable under physiological conditions. However in the presence of the targeted nucleic acid it must unfold in order to permit the ODN to form a perfect duplex with the target. The investigation of these ODN structures has been started, especially for phosphorothioates (18-20). Non-modified phosphodiester ODNs are less studied.

In the present work, the target recognition ability and nuclease resistance of ODNs with the natural phosphodiester backbone and different secondary structure (linear, hairpin, looped, snail-like) are investigated. All ODNs under study have a 21-member fragment complementary to the translation initiation region of *env* RNA of the Friend murine leukaemia retrovirus (FIG. 1).

## MATERIALS AND METHODS

### Oligonucleotides.

All oligonucleotides were purchased from Eurogentec (Seraing, Belgium), additionally desalted on G25 Sephadex Columns and quantitated by absorbance at 260 nm.

### Protection of 5'-terminal phosphate of the antisense oligonucleotides.

5'-Terminal labelling of the oligonucleotides was performed using [ $\gamma$ - $^{32}$ P]-ATP (Amersham) and T4 polynucleotide kinase (Promega). The labelled oligonucleotides were purified by electrophoresis in a 20% denaturing polyacrylamide gel. In order to protect the terminal [ $^{32}$ P]-phosphate against enzymatic digestion the modified method of carbodiimide condensation (21) was used. The oligonucleotides were dissolved in

Target sequences

D	5'-d (CCAGC <u>AGAATCGACACATGGCGTGTTC</u> ACGCT)-3'
R	5'-r (CCAGCAGAAUCGACACAUGGCGUGUUAACGCU)-3'

Antisense oligodeoxynucleotides

21L	5'-TGAACACGCCATGTCGATTCT-3'
55L	5'-T <sub>2</sub> ACT <sub>3</sub> CT <sub>5</sub> GCGTTGAACACGCCATGTCGATTCTT <sub>5</sub> CT <sub>5</sub> C <sub>6</sub> -3'
21PS	5'-T*G*AAACACGCCATGTCGATTCT-3'
H6	5'-TGAACACGCCATGTCGATTCT <sub>T</sub> 3'-CTAAGAT <sub>T</sub>
H8	5'-TGAACACGCCATGTCGATTCT <sub>T</sub> 3'-AGCTAAGAT <sub>T</sub>
H10	5'-TGAACACGCCATGTCGATTCT <sub>T</sub> 3'-ACAGCTAAGAT <sub>T</sub>
Dh6	<sub>C</sub> TGAACACGCCATGTCGATTCT <sub>T</sub> <sub>T</sub> ACTTGT-5' 3'-CTAAGAT <sub>T</sub>
L8	5'-GCGTA <sub>T</sub> GAA <sup>ACGC</sup> <sub>C</sub> 3'-CGCAT <sub>T</sub> CTT <sub>A</sub> GCTG <sub>T</sub>
L10	5'-GCGCTTA <sub>T</sub> GAA <sup>ACGC</sup> <sub>C</sub> 3'-CGCGAAT <sub>T</sub> CTT <sub>A</sub> GCTG <sub>T</sub>
SL	<sub>T</sub> C TGAACACGCCATGTCGATTCT <sub>T</sub> <sub>T</sub> AGCCGGGGCCGGGCTCCGGTT-β-5'- <sub>T</sub> T 3'-α-TCGGCCCCGGCCCCGAGGCCAA- <sub>T</sub>

FIG. 1. Oligonucleotides used in the study. 21-member targeted RNA and DNA sequences are underlined. Sequences of antisense oligodeoxyribonucleotides complementary to the D and R targets are typed in bold.  
\*-phosphorothioate group.

100  $\mu$ l of 1 M N-methylmorpholine buffer (pH 7.5), 20 mM  $\text{MgCl}_2$  containing 50% of ethanol and the solutions were supplemented by 10 mg of 1-ethyl-3(3'-dimethylaminopropyl)carbodiimide. The reaction proceeded for 16 h at 4°C and the oligonucleotide ethyl esters were twice precipitated with 1 ml of 2% solution of  $\text{LiClO}_4$  in acetone, washed by acetone and further mixed with the non-labelled ODNs and used to study their resistance to enzymatic digestion.

### Thermal denaturation experiments.

Absorbance vs. temperature curves were recorded at 260 nm using a Uvikon 933 spectrophotometer equipped with thermoprogrammer. The ODN solutions were prepared in 600  $\mu$ l of a 10 mM Na-phosphate buffer (pH 7.5) with 50 mM NaCl. The concentration of each oligonucleotide strand was  $10^{-6}$  M. Absorbance was monitored while temperature was raised at a rate of 0.5°C/min from 20°C to 80°C. Melting temperatures ( $T_m$ ) were determined by computer fit of the first derivative of absorbance with respect to  $1/T$ . Uncertainty in  $T_m$  is estimated at  $\pm 0.5^\circ\text{C}$  based on repetitions of experiments. Free energy values for the duplex dissociation were derived by computer-fitting the melting curves, using the two-state model (22).

### Native gel electrophoresis.

The RNA and DNA templates (**R** and **D**) were labelled using [ $^{32}\text{P}$ - $\gamma$ ]-ATP and T4 polynucleotide kinase. The oligonucleotides (10 pmol of each strand) were dissolved in 10  $\mu$ l of the 10 mM Tris-acetate buffer (pH 7.5), 150 mM  $\text{CH}_3\text{COONa}$ , 2 mM  $\text{MgCl}_2$  and incubated at 37°C for one hour and then supplemented with 1  $\mu$ l of 70% glycerol containing xylene cyanol and bromophenol blue. Electrophoresis was performed in a non-denaturing 15% acrylamide gel (19:1 acrylamide/bis-acrylamide) in the same Tris-acetate buffer at 37°C for 24 h (9 V/cm).

### RNase H-mediated cleavage.

In order to study RNase H triggering activity of the ODNs, they (10 pmol) were mixed with the 5'-[ $^{32}\text{P}$ ]-labelled RNA template (**R**) (1 pmol) in 10  $\mu$ l of 20 mM Tris-HCl buffer (pH 7.5), 10 mM  $\text{MgCl}_2$ , 100 mM KCl, 0.1 mM DTT in the presence of 0.5  $\mu$ l of RNasin (Gibco BRL) and incubated for 30 min at 37°C. Then 0.5 U of *E.coli* RNase H

(Promega, Madison, WI) were added and the mixtures were incubated at 37°C for 15 min. The samples were then precipitated with acetone containing 2 % of LiClO<sub>4</sub>, dried, dissolved in 4 µl of formamide:water (4:1), 0.01 % bromophenol blue, and 0.01 % xylene cyanol and analysed by electrophoresis in a 20 % denaturing polyacrylamide gel with a following autoradiography.

### **Cells and media.**

NIH 3T3 and HeLa cell lines were grown in DMEM medium supplemented with 5% and 10% of heat inactivated foetal bovine serum (FBS) (Gibco BRL), respectively, streptomycin (100µg/ml) and penicillin (100U/ml). All cell lines were incubated at 37°C in 5% CO<sub>2</sub>.

### **Transfecting agent.**

In order to deliver ODNs inside the cells SuperFect™ was used. It is a dendrimeric structure presenting 140 terminal NH<sub>2</sub> groups on its surface, sixty of them are positively charged at pH 7. Its molecular weight is 35 kD. SuperFect™ concentration used for cellular experiments was 3mg/ml.

### **Preparation of cell lysates.**

HeLa and NIH 3T3 cells were washed three times with phosphate saline buffer (PBS) and then scraped into 1 ml of 10 mM Na-phosphate buffer (pH 7.5), 10 mM MgCl<sub>2</sub>, 150 mM NaCl, 1 mM DTT, 1% NP-40, 0.2 mg/ml phenyl-methylsulphonyl fluoride (PMSF) and kept at -20°C for 30 min. After defrost the cells were centrifuged at 14000g for 15 min at 4°C. The supernatants were used to study enzymatic degradation of the oligonucleotides. Protein concentration in each lysate was quantitated using bovine serum albumin (BSA) as a standard (23).

### **Study of oligonucleotide degradation in biological media.**

Determination of the rate of the oligonucleotide nuclease degradation was carried out in DMEM containing 10% heat inactivated FBS (56°C for 30 min) and prepared cell lysates. The lysates were diluted by 10 mM Na-phosphate buffer (pH 7.5), 10 mM mgCl<sub>2</sub>, 150 mM NaCl, 1 mM DTT in order to have the same total protein concentration equal to 1.22 mg/ml. To avoid the enzymatic [<sup>32</sup>P]-labelled phosphate

cleavage, the oligonucleotides with the protected terminal phosphate prepared as described above were used. The [ $^{32}\text{P}$ ]-labelled ODNs in 10  $\mu\text{M}$  concentration were incubated in 120  $\text{rL}$  of the corresponding *medium* at 37°C. At various times, 15  $\text{rL}$  aliquots were removed, supplemented by 15  $\mu\text{L}$  of 50 mM EDTA and frozen at -20°C. The samples were twice extracted with phenol:chloroform:*iso*-amyl alcohol (25:24:1). The oligonucleotides were precipitated from aqueous fractions by 10 volumes of acetone containing 2% of  $\text{LiClO}_4$ , dried, and dissolved in 5  $\text{rL}$  of formamide:water (4:1), 0.01 % bromophenol blue, and 0.01 % xylene cyanol. Samples were analysed by electrophoresis in a 20 % denaturing polyacrylamide gel. Resulting gels were scanned using the phosphorimager (Storm 840, Molecular Dynamics). Degradation of oligonucleotides was quantitated as a ratio of the signal efficiency of bands corresponding to intact and degraded oligonucleotides. Uncertainty in degradation percent is estimated at  $\pm 5\%$  based on repetitions of experiments.

### Study of oligonucleotide degradation inside the cells.

The day before, cells were seeded on 6-well plates to obtain 60-80% of confluence ( $4 \times 10^5$  cells). 5  $\mu\text{g}$  of each ODN were mixed with 6  $\mu\text{L}$  of SuperFect<sup>TM</sup> (3mg/ml) (Qiagen, Canada) in a final volume of 150  $\mu\text{L}$  of DMEM (without FBS and antibiotics) for 10 min at room temperature. Cells were washed with PBS, the SuperFect<sup>TM</sup>-ODN mixtures were diluted with 850  $\mu\text{L}$  of 10% (for HeLa cells) or 5% (for NIH 3T3 cells) FBS DMEM (with antibiotics) and added on cells.

The supernatant was removed after 16 or 48 hours, and the cells were harvested by trypsin treatment. Then the cells were washed three times with PBS, suspended in 500  $\mu\text{L}$  of 10 mM Na-phosphate buffer (pH 7.5), 150 mM NaCl, 20 mM EDTA, 1% NP-40 and kept at -20°C for 30 min. After defrost the cells were heated at 90°C for 30 min in order to destroy completely all cellular compartments and twice extracted with phenol:chloroform:*iso*-amyl alcohol (25:24:1). The ODNs were precipitated from the aqueous fractions containing 0.3 M Na-acetate by adding 5-fold excess of ethanol, dissolved in 5  $\text{rL}$  of formamide:water (4:1), 0.01 % bromophenol blue, and 0.01 % xylene cyanol and analysed by electrophoresis in 20% denaturing gel. Resulting gels were scanned using the phosphorimager (Storm 840, Molecular Dynamics). Degradation of oligonucleotides was quantitated as a ratio of the signal efficiency of bands corresponding to intact and degraded oligonucleotides.

## RESULTS

### Design of oligonucleotides.

All studied oligodeoxyribonucleotides have a 21-member sequence 5'-TGAACACGCCATGTCGATTCT-3' complementary to the translation initiation region of *env* RNA of the Friend murine leukaemia retrovirus (**FIG. 1**). Oligonucleotides **21L** and **55L** have a linear structure as well as the oligonucleotide **21PS**. However, the latter contains two phosphorothioate groups at both ends in order to protect it from the enzymatic degradation. **H6**, **H8** and **H10** have different numbers of base pairs (b.p.) in the stem region of hairpins located at their 3'-end. **Dh6** can form a hairpin structure with two 6 b.p. stems at both 3'- and 5'-ends. **L8** and **L10** can form a looped structure with 13 nucleotides situated in the loop and stems with 8 and 10 b.p., respectively. A snail-like structure **SL** is formed by a chimerical  $\alpha$ - $\beta$ -oligonucleotide containing at the 3'-end an  $\alpha$ -nucleotide sequence complementary to its 5'-end  $\beta$ -nucleotide sequence. Since  $\alpha$ -ODNs specifically form parallel duplexes with complementary  $\beta$ -ODNs instead of antiparallel ones, the 3'-end  $\alpha$ -sequence of the chimerical  $\alpha$ - $\beta$ -oligonucleotide forms a stable parallel duplex with its 5'-end  $\beta$ -sequence. The inner part of the oligonucleotide forms a circle-like structure.

### Investigation of the binding properties of structured oligonucleotides.

The  $T_m$  (melting temperature) and the  $\Delta G_{37}^0$  (duplex formation energy) are determined both for structured oligonucleotides alone and for their complexes with complementary DNA (**D**) or RNA (**R**) targets (**TABLE**). The thermostability of inner duplexes in ODNs **H6-H10**, **L8** and **L10** depends on the number of base pairs in their stem regions. Nevertheless, all SODNs are able to interact with both DNA and RNA targets forming intermolecular duplexes having different thermodynamic parameters than the intramolecular duplexes (**TABLE**). The  $T_m$  found for these bimolecular duplexes differ from the  $T_m$  of the SODNs and correspond approximately to the  $T_m$  detected for the duplexes formed by the linear ODN **21L** with both targets. A slight  $T_m$  decrease found for **Dh6**, **L10** and especially for **SL** may be explained by destabilising effect of two unpaired extremities in duplexes of these ODNs with both targets. The melting curves of all SODNs in presence of both RNA and DNA targets have one transition corresponding to their intermolecular duplexes denaturation. The only exception is the oligonucleotide **H10** which displays a very stable hairpin



**TABLE.** Thermodynamic parameters<sup>(a)</sup> for oligonucleotide duplexes. Data obtained in 10 mM phosphate, 50 mM NaCl, pH 7.5. Oligonucleotide concentration  $10^{-6}$  M.

Systems	$T_m$ (°C)	$-\Delta H^\circ$ (kcal mol <sup>-1</sup> )	$-\Delta S^\circ$ (e.u.)	$-\Delta G^\circ_{(37)}^{(b)}$ (kcal mol <sup>-1</sup> )
<b>21L+D</b>	60	101	267	18
<b>21L+R</b>	57	105	286	16
<b>21PS+D</b>	60	82	215	15
<b>21PS+R</b>	57	86	232	14
<b>H6</b>	52	45	139	2
<b>H6+D</b>	58	92	249	15
<b>H6+R</b>	56	82	222	13
<b>H8</b>	66	62	190	3
<b>H8+D</b>	60	60	151	13
<b>H8+R</b>	56	52	130	12
<b>H10</b>	75	44	128	4
<b>H10+D</b>	43, 60, 73	43	102	11
<b>H10+R</b>	40, 57, 73	35	78	11
<b>Dh6</b>	52	35	104	3
<b>Dh6+D</b>	57	90	245	14
<b>Dh6+R</b>	55	80	218	12
<b>L8</b>	47	46	142	2
<b>L8+D</b>	60	96	260	15
<b>L8+R</b>	57	101	280	14
<b>L10</b>	53	68	208	3
<b>L10+D</b>	57	94	255	15
<b>L10+R</b>	55	96	265	14
<b>SL</b>	65	43	128	3
<b>SL+D</b>	55	70	182	14
<b>SL+R</b>	53	65	176	10

<sup>(a)</sup>  $\Delta H^\circ$ ,  $\Delta S^\circ$  and  $\Delta G^\circ$  are the average of several values obtained from independent melting curves and are expressed as round numbers. Estimated errors in  $\Delta H^\circ$ ,  $\Delta S^\circ$ ,  $\Delta G^\circ$  and  $T_m$  are  $\pm 4\%$ ,  $\pm 4\%$ ,  $\pm 8\%$  and  $\pm 1\%$ , respectively.

<sup>(b)</sup>  $\Delta G^\circ_{37} = \Delta H^\circ - (310 \times \Delta S^\circ)$ .

( $T_m=75^\circ\text{C}$ ). In the presence of **D** or **R** targets the melting curve has three transitions: the first one may correspond to the melting of a partial intermolecular duplex formed between the 11-member single stranded fragment of this ODN and the target ( $43^\circ\text{C}$  with the DNA target and  $40^\circ\text{C}$  with the RNA), the second one to the melting of the complete intermolecular duplex ( $60^\circ\text{C}$  with the DNA target and  $57^\circ\text{C}$  with the RNA) and the third one to the melting of its own double helice domain ( $73^\circ\text{C}$ ). In order to calculate the thermodynamical parameters the formation of intermolecular duplexes between the SODNs and both targets is considered as two-step process: unfold of the intramolecular duplexes and hybridisation of unfolded ODNs with their target. So  $\Delta G$  corresponding to the formation of intermolecular duplexes represent the sum of  $\Delta G$  corresponding to the unfold of inner duplexes and  $\Delta G$  of intermolecular duplexes listed in the table. These summary  $\Delta G$  are close to  $\Delta G$  calculated for the duplexes between **21L** and **R** or **D** targets. In the of **H10** which really displays 3 transitions we can calculate only approximate  $\Delta G$  regarding its melting curve as a curve with one transition.

The binding of the SODNs with the RNA and DNA targets is also studied by a gel mobility shift assay (**FIG. 2**). The ODNs are incubated with [ $^{32}\text{P}$ ]-labelled targets **D** and **R** at  $37^\circ\text{C}$  and the mobility of the complexes formed is determined by electrophoresis in a 15% non-denaturing polyacrylamide gel. **FIG. 2** shows that the electrophoretical mobility of the both targets changes in the presence of all SODNs as a result of their involvement into the formation of corresponding duplexes. Unfortunately a band of the [ $^{32}\text{P}$ ]-labelled RNA (**FIG. 2A**, lane 1) is very dispersive, probably, due to formation of some intramolecular hairpins by this oligoribonucleotide. However in presence of all complementary ODNs clear bands corresponding to their intermolecular duplexes with the RNA target are detected. It should be noted that **SL** shows two retarded bands with both RNA and DNA targets (**FIG. 2A,B**, lane 10). The upper band corresponds to the intermolecular duplex with an unfold form of **SL** and the lower one likely to be the complex in which the inner duplex also exists, at least partially. The structure of this complex is more compact, so its electrophoretical mobility is higher.

The ability of SODNs to hybridise to the complementary RNA strand and to trigger the RNase H-mediated cleavage of the RNA is also investigated. **FIG. 3A** shows the results of incubation of the RNA target ( $0.1\ \mu\text{M}$ ) and various ODNs (1

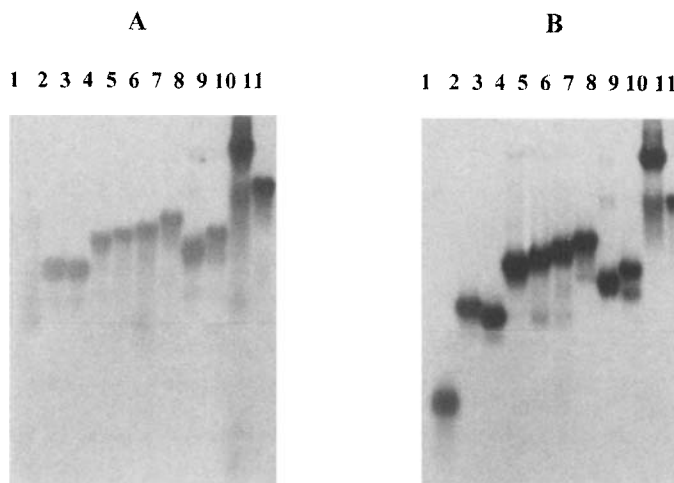


**FIG. 2.** Electrophoretic analysis of duplex formation in a 15% native PAGE at 37°C.  
**A.** Binding of the [ $^{32}$ P]-labelled RNA target (lane 1) to the oligonucleotides: **21L** (lane 2), **21PS** (lane 3), **H6** (lane 4), **H8** (lane 5), **H10** (lane 6), **Dh6** (lane 7), **L8** (lane 8), **L10** (lane 9), **SL** (lane 10), **55L** (lane 11).  
**B.** Binding of the [ $^{32}$ P]-labelled DNA target (lane 1) to the oligonucleotides: **21L** (lane 2), **21PS** (lane 3), **H6** (lane 4), **H8** (lane 5), **H10** (lane 6), **Dh6** (lane 7), **L8** (lane 8), **L10** (lane 9), **SL** (lane 10), **55L** (lane 11).

$\mu$ M) with 0.5 unit of RNase H at 37°C for 15 min. All ODNs are found to form with the RNA **R** duplexes which are substrates for RNase H. The RNA cleavage by RNase H in presence of the linear oligonucleotide **21L** and all SODNs occurs at the same sites. The major cleavage sites are indicated by arrows in **FIG. 3B**. In the absence of complementary ODNs no cleavage of the RNA is observed.

All these results show that the inner double stranded structure of the ODNs does not prevent them to interact with their DNA and RNA targets. The inner duplexes seem to dissociate when the bimolecular complexes between the SODNs and their targets are formed. Evidently, this is true if these bimolecular duplexes are thermodynamically preferable (**TABLE**).

#### Stability of antisense oligonucleotides to nucleolytic degradation.

The ability of the structured ODNs to resist to the enzymatic hydrolysis is studied in DMEM supplemented with 10% of heat inactivated foetal bovine serum

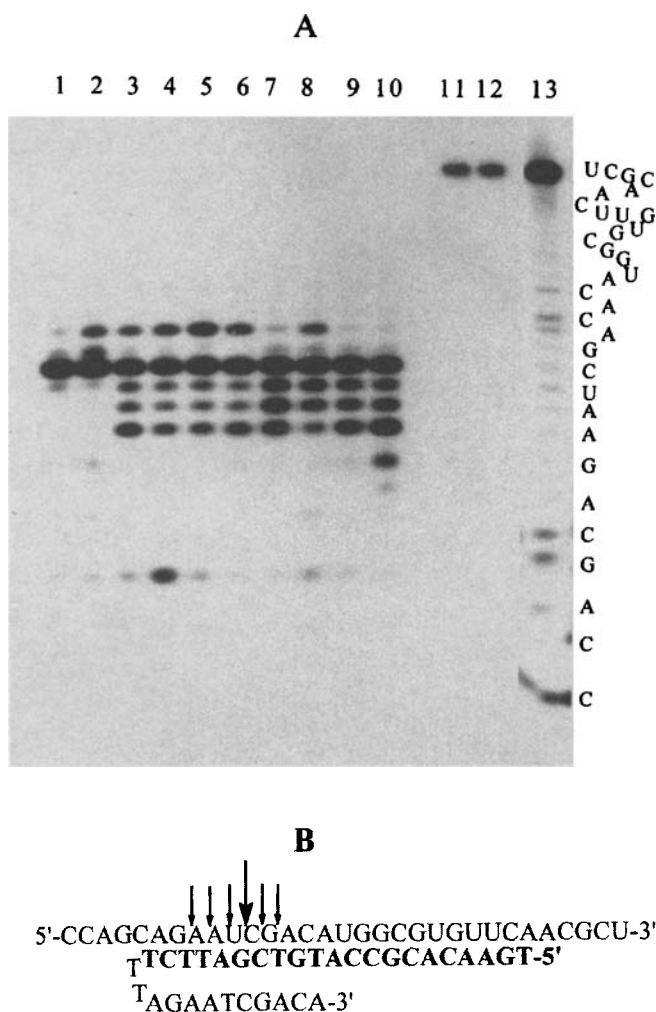


**FIG. 3. A.** Cleavage of the RNA target by RNase H in the presence of antisense oligonucleotides: **21L** (lane 1), **21PS** (lane 2), **H6** (lane 3), **H8** (lane 4), **H10** (lane 5), **Dh6** (lane 6), **L8** (lane 7), **L10** (lane 8), **SL** (lane 9), **55L** (lane 10). [ $^{32}$ P]-labelled RNA **R** alone (lane 11); **R** in the presence of RNase H without ODNs (lane 12); **R** hydrolysis under alkaline conditions (lane 13).

**B.** Schematic presentation of the duplex formed between the RNA target and **H10**. Arrows show the major cleavage sites.

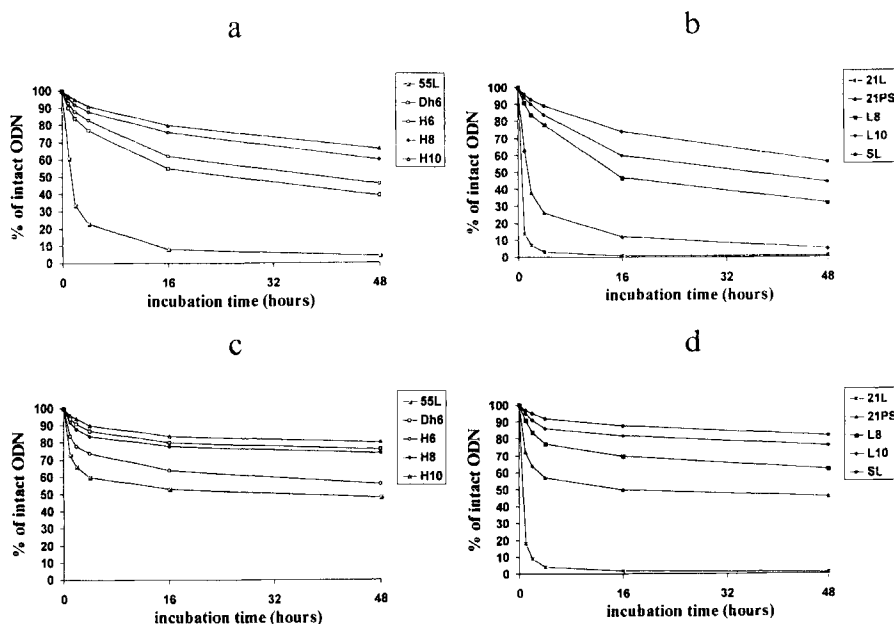


**FIG. 4.** Degradation of the antisense oligonucleotides in DMEM supplemented with 10% heat-inactivated FBS in the absence (**a,b**) and in the presence (**c,d**) of SuperFect<sup>TM</sup>.

(FBS) widely used to grow cells as well as in cellular lysates and two types of cell lines: NIH 3T3 and HeLa. To avoid the enzymatic [<sup>32</sup>P]-labelled phosphate cleavage, oligonucleotides with the 5'-terminal phosphate protected by ethyl residue are used for this study.

The investigation of the ODN degradation in the culture medium containing FBS demonstrates that hairpin, looped and snail-like structures increase significantly the nuclease resistance of the SODNs (**FIG. 4a,b**). The resistance of hairpin and looped ODNs to nucleolytic degradation depends on the type of inner duplexes and their thermal stability. For example, the half-life of the most thermostable hairpin **H10** is higher than for hairpins **H6** and **H8**. At the same time the looped ODN **L10** is as resistant to the degradation as the hairpin **H8** whereas its thermal stability is lower (53°C for **L10** and 66°C for **H8**). All linear oligonucleotides **21L**, **55L** and **21PS** are rapidly degraded. These results confirm the previously reported data concerning the very short half-life of linear phosphodiester and phosphorothioate capped oligonucleotides in serum (4, 24).

In order to improve the oligonucleotide uptake into cells several transfecting reagents can be utilised (25-29). The influence of one of them, a dendrimeric molecule named SuperFect<sup>TM</sup>, on the ODN stability in DMEM supplemented with 10% of FBS is investigated in our work. Complexes formed by the ODNs with SuperFect<sup>TM</sup> are found to be more resistant to the nucleolytic degradation than the ODNs alone (**FIG. 4c,d**). The resistance increase is the most significant for the linear ODNs **55L** and **21PS**. For example, the half-life of the phosphorothioate capped ODN **21PS** with SuperFect<sup>TM</sup> and without it is about 12 hr and 30 min, respectively. The similar increasing of the nucleolytic stability is observed for **55L** (**FIG. 4a,c**). This is in agreement with previous literature data shown that the formation of complexes of polyamine compounds with ODNs increases their nuclease stability (25). At the same time the half-life of the nonmodified **21L** with and without SuperFect<sup>TM</sup> is about the same. Possibly the complex formed by SuperFect<sup>TM</sup> with this short ODN does not protect sufficiently the ends of the oligonucleotide that undergo the enzymatic cleavage.

Stability of ODNs in lysates of HeLa and NIH 3T3 cell lines varies with the lysate type. Notice that the total protein concentration in these lysates is the same. Therefore the distinctions between their nucleolytic activities depends on either quantitative or qualitative differences in the nuclease activities. The degradation is more rapid in the HeLa lysate (**FIG. 5a,b**). The snail-like ODN **SL** having a half-life of about 3 h is much more resistant than other SODNs. All linear ODNs (**21L**, **21PS** and **55L**) are rapidly degraded (their half-life is about 10 min).

Concerning the NIH 3T3 lysate, the rate of the SODN degradation is much lower when compared to the HeLa lysate (**FIG. 5c,d**). Interestingly, the SODNs **Dh6**, **L8**, **L10** and **SL** with both 5'- and 3'-end protection are more stable than the SODNs **H6-H10** having only 3'-end hairpins. This fact allows one to suggest that the contribution of 5'-exonuclease activity in the ODN degradation is very important in this lysate. Nevertheless, terminal phosphorothioate modification has no significant influence on the ODN resistance (compare **21L** and **21PS** ODNs).

The fate of the ODNs in two cell lines, HeLa and 3T3, is also investigated (**FIG. 6**). To improve the ODN penetration into the cells, their complexes with the transfecting reagent SuperFect<sup>TM</sup> are preliminary formed and incubated with cells. ODN **21L** is not studied because even in presence of SuperFect<sup>TM</sup> it is very rapidly digested in the biological *medium* used for the cell incubation (**Fig. 4**). Significant

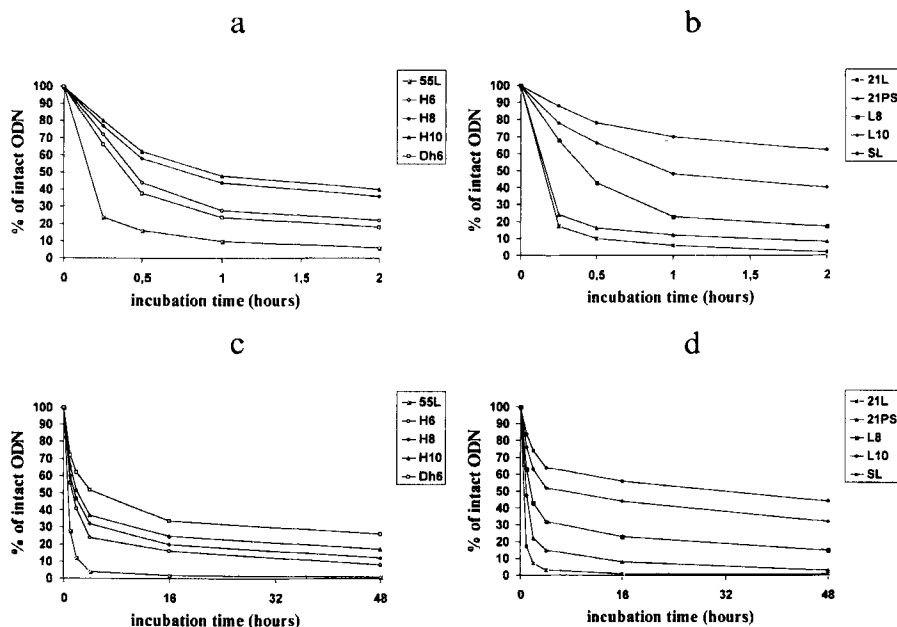


**FIG. 5.** Degradation of the antisense oligonucleotides in cellular lysates: (a,b) HeLa lysate, (c,d) NIH 3T3 lysate.

quantities (50-80%) of other ODNs including the linear ones (**55L** and **21PS**) are detected in the cells (**FIG. 6a-d**). After 48 h of incubation the amount of intact ODNs inside the cells decreases but remains at the level of 20-30%. There is no significant difference between both cell lines (**FIG. 6 a,b** and **c,d**). All structured ODNs have about the same stability that is superior to the stability of the linear ODNs **55L** and **21PS**.

## DISCUSSION

The modulation of gene expression is one of the most promising pharmaceutical applications of ODNs. Among the most important properties that antisense ODNs have to fulfill are the resistance to nucleolytic digestion and the ability to bind selectively to the target RNA molecule forming a substrate efficiently hydrolysed by RNase H. ODNs with a natural phosphodiester backbone form with RNA targets an efficient substrate for RNase H but, unfortunately, they are quickly degraded in biological media by numerous nucleases. In the present study, nonmodified oligodeoxyribonucleotides forming looped, hairpin and snail-like inner secondary

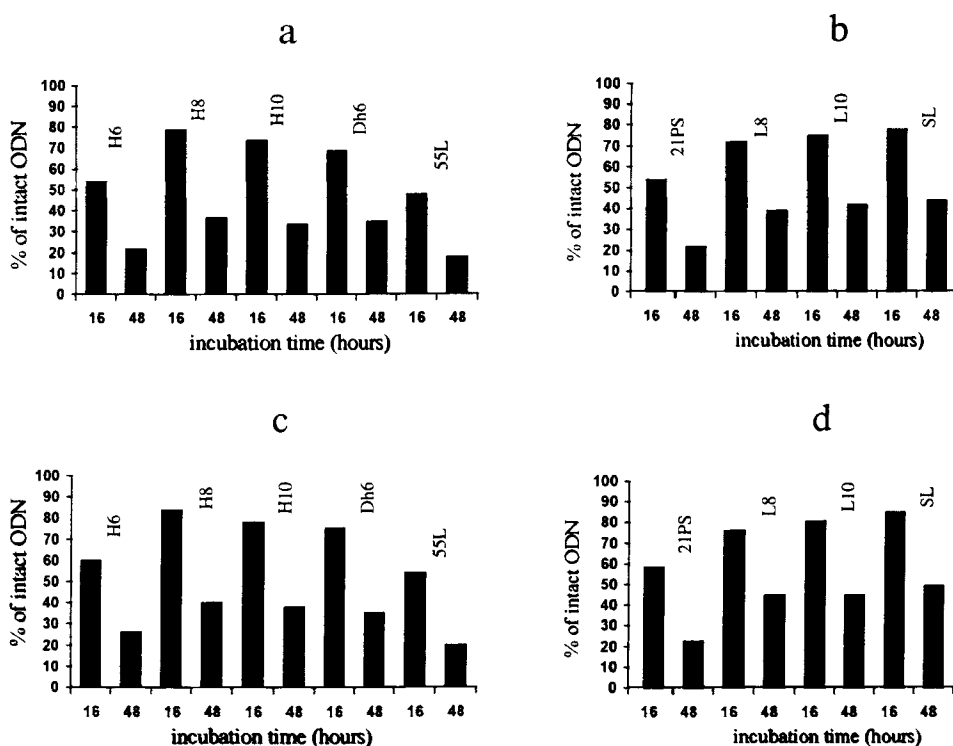


**FIG. 6.** Degradation of the antisense oligonucleotides complexed with SuperFect™ inside cells: (a,b) HeLa, (c,d) NIH 3T3 cells.

structure are studied for their ability to interact with their targets and their resistance to nuclease digestion.

All ODNs contain a 21-mer sequence complementary to the translation initiation region of *env* RNA of the Friend murine leukaemia retrovirus. However, this sequence is partially involved in formation of inner duplexes resulting in hairpin (H6-H10, Dh6), looped (L8, L10) or snail-like (SL) secondary structure of the ODNs (FIG. 1). The main challenge of the structured ODNs design is to choose the structure of the inner duplexes in such a way that the ODN interaction with their targets should not be prevented. For this purpose the ODNs with a different length of their double stranded stem (H6-H10 and L8, L10) are studied. Furthermore, the influence of the linear ODN length (21L, 55L) on their resistance to nucleolytic degradation is also investigated.



To study the structured ODNs (SODNs) ability to hybridise to their DNA (**D**) and RNA (**R**) targets, thermal denaturation experiments, native gel assays and RNase H treatments are used. All these methods show that the designed SODNs can recognise both targets and form duplexes with them. Moreover, the  $T_m$  of these intermolecular duplexes are approximately the same as the  $T_m$  of the duplexes formed by the linear 21-mer (**21L**). These results as well as the pattern of the RNA target hydrolysis by RNase H in the hybrid duplexes made by all SODNs allow us to propose that the SODNs generate perfect 21 base pair duplexes with the targets. It means that the formation of the intermolecular duplexes leads to denaturation of the SODN inner secondary structure. The slight decrease of the intermolecular duplex thermal stability observed for some SODNs (**Dh6**, **L10** and **SL**) when compared to the corresponding linear duplex may be explained by either the influence of two unpaired extremities of these ODNs or a partial retention of their inner duplexes (especially for **SL**). The intermolecular duplex formation energy values ( $\Delta G^\circ$ ) are less for the SODNs if compared with the linear **21L**. It reflects the price to pay to unfold their inner structures and shows that the SODNs are weaker binders than linear ODNs. However this effect makes the SODNs more sensitive to any mismatches in targeted nucleic acids and, therefore, more specific as antisense reagents.

The effect of the SODN secondary structure on their resistance to enzymatic hydrolysis is investigated using one culture medium (DMEM supplemented with 10% of heat inactivated foetal bovine serum), two cellular lysates and two types of cell lines: murine fibroblast (NIH 3T3) and human epitheloid carcinoma (HeLa). The choice of a fragment of *env* RNA of the Friend murine leukaemia retrovirus as a target of the studied ODNs conditions the use of murine fibroblasts NIH 3T3. It is known that the efficacy of antisense ODNs may vary considerably according to the cell type. In consequence, it is interesting to compare these cells with HeLa cells, coming from a human epitheloid carcinoma and widely used for antisense experiments. Lysates of these cells are also utilised.

All ODNs contain [ $^{32}\text{P}$ ]-labelled 5'-terminal phosphate protected by ethyl residue. It allows us to avoid the enzymatic dephosphorylation of the ODNs and observe their real degradation by nucleases. The patterns of ODN hydrolysis are found to vary significantly in the different biological *media*. **FIG. 7** represents the results of one of the SODNs degradation in DMEM (**FIG.7A**) and both cellular lysates (**FIG.7B,C**).

Foetal bovine serum (FBS) is known to contain a significant 3'-exonuclease activity (30, 31). Therefore it is not surprising that ODNs having 3'-hairpins (**H6-H10** and **Dh6**) are much more stable in DMEM supplemented with 10% of heat inactivated FBS than the linear ones (**21L** and **55L**) (**FIG. 4a,b**). The increase of the hairpin thermostability generally increases the nucleolytic resistance of the SODNs. However, it is important to note that the nucleolytic resistance depends on both the thermostability of the ODN inner duplex and the secondary structure type. Thus, the looped ODN **L10** is as resistant to enzymatic hydrolysis in DMEM as the hairpin **H8** whereas the latter has a more stable inner duplex (compare  $T_m$  66°C for **H8** and 53°C for **L10**). Two phosphorothioate groups situated at both ends of the linear ODN **21PS** do not really protect it from the nuclease hydrolysis (**FIG. 4b**).

The SODN fate in the cellular lysates depends substantially on the lysate source (**FIG. 5a-d**). In the murine fibroblast (NIH 3T3) lysate the SODNs having both extremities involved in the inner structure formation (**Dh6**, **L8**, **L10** and **SL**) are more stable than the SODNs **H6-H10** containing only 3'-hairpins (**FIG. 5c,d**). This result permits to conclude that a 5'-nuclease activity is important in these cell lines for the ODN degradation. Comparison of the patterns of Dh6 degradation in DMEM and NIH 3T3 lysate (**FIG. 7A,B**) confirms this conclusion. Indeed, in the NIH 3T3 lysate we can not see shortened oligonucleotide products typical for the 3'-exonuclease digestion, the 5'-[ $^{32}$ P]-labelled nucleotide (or its ethyl ester) is the major hydrolysis product. The ODNs are much more actively degraded in HeLa than in 3T3 lysate (**FIG. 5a,b**). Besides, the enzymatic hydrolysis in the HeLa lysate results mainly in the appearance of products having the length of 15-20-mers (**FIG. 7C**). This suggests that the predominant nuclease activity in this system may be endonucleolytic. The snail-like ODN **SL** is more stable in this lysate than the other ones (**FIG. 5b**), probably, because the single stranded part, which is the most sensitive to endonuclease hydrolysis, is partially protected in space by the duplex part of this ODN which is very close.

An important part of this investigation is devoted to the study of the nuclease resistance of SODNs in the presence of SuperFect<sup>TM</sup>. This reagent has a dendrimeric structure with numerous positive charges situated on the molecule surface. Dendrimers are currently being developed as new delivery agents for DNA transfections (32). This structure is able to complex nucleic acids by electrostatic interactions, and once inside the cell, to act as a buffer in the endosomal compartment (33). Previous results

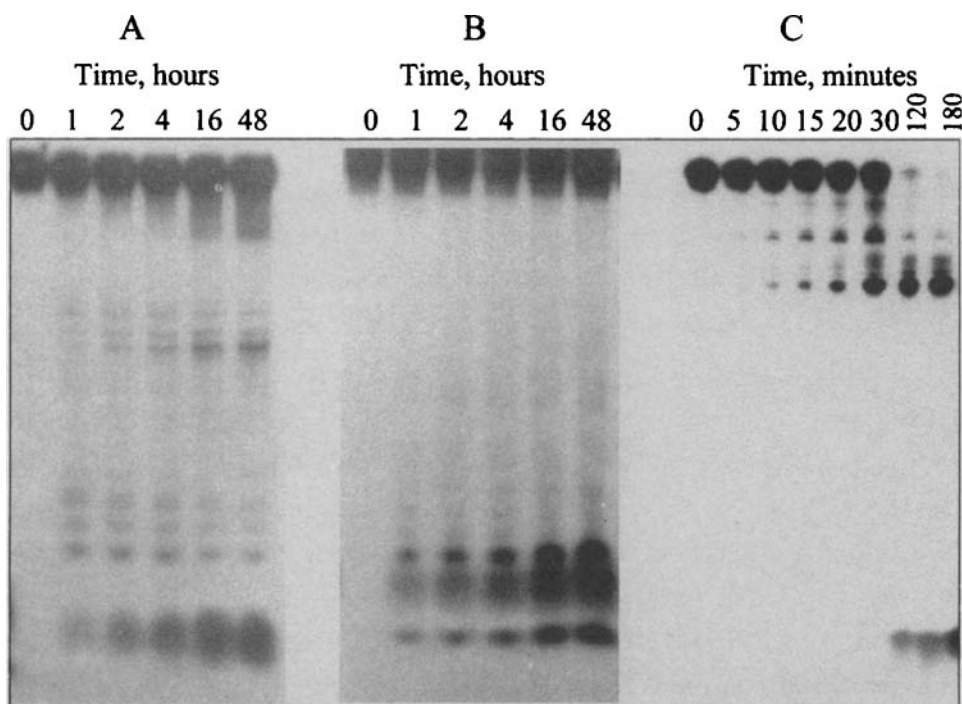


**FIG. 7.** Electrophoretic analysis of **Dh6** degradation in DMEM supplemented with 10% of FBS (A), NIH 3T3 lysate (B) and HeLa lysate (C).

obtained with such complexes have shown that their use enhances plasmid DNA expression in tissue cultures (32), improves delivery of antisense ODNs (27, 29) and facilitates inhibition of specific gene expression (32, 34). Earlier we have shown that SuperFect<sup>TM</sup> improves considerably the ODN penetration in HeLa and NIH 3T3 cells (in press). In this work we study the influence of this reagent on the ODN enzymatic stability in DMEM supplemented by 10% of FBS used in our experiments to grow these cells (**FIG. 4c,d**). SuperFect<sup>TM</sup> is found to increase significantly the ODN resistance to nuclease digestion. It is not surprising because formation of the complex with polycation particles decreases the ODN accessibility to nucleases. However, one result must be emphasised especially: the linear phosphodiester **55L** acquires an enhanced resistance whereas the linear **21L** does not. It means that the ODN interaction with SuperFect<sup>TM</sup> based on the electrostatic forces depends to a considerable extent on the ODN length, and the complex with the 21-mer is too weak

in order to protect it. On the other side, another 21-mer having two phosphorothioate groups at both extremities (**21PS**) becomes resistant to nucleases in the presence of SuperFect<sup>TM</sup>. To explain this fact we can propose the following hypothesis: the complex between SuperFect<sup>TM</sup> and 21-mer ODNs is formed but it is rather weak and nucleases can hydrolyse at least oligonucleotide extremities. Owing to this hydrolysis the size of the ODN is reduced and this results in denaturation of the complex. However, if ODN ends are modified, it prevents them from nuclease action and the ODN remains intact.

Based on these results, one important conclusion may be drawn. SuperFect<sup>TM</sup> can not be applied for antisense ODNs usually containing 15-20 nucleotides if they are not at least end modified. Another possibility is to use extended ODNs but, unfortunately, they will be less specific. In order to regain the specificity, their single stranded part responsible for the target recognition has to be shortened. This may be obtained by using structured ODNs.

Investigation of the ODN fate inside the NIH 3T3 and HeLa cells shows that all ODNs complexed with SuperFect<sup>TM</sup>, except the phosphodiester 21-mer, are rather stable. The ODN **21L** stability inside the cells is not studied because of its very rapid hydrolysis in DMEM. The similar stability of ODNs in both cell lines is likely conditioned by their protection with SuperFect<sup>TM</sup> because their intrinsic stability in the lysates of these cells is quietly different.

Summarising the results of this investigation we can conclude that phosphodiester oligonucleotides might be efficiently applied in antisense technology with carrier agents. However they must be rather extended (at least more than 30-mer) in order to form stable complexes with transfecting agents. On the other side, they must form some inner secondary structure in order to reduce their single stranded part responsible for the specific recognition of the RNA target. Double stranded part of structured ODNs must be rather stable under physiological conditions but has not to prevent them from the ODN unfolding and hybridisation to their DNA and RNA targets. Evidently, ODNs having looped or snail-like structure are in general more resistant to nuclease degradation than ODNs forming only 3'-end hairpins.

## ACKNOWLEDGEMENTS

We acknowledge Dr. B. Rayner for the synthesis of the chimeric  $\alpha$ - $\beta$ -oligonucleotide and Dr. O. Sidorkina for valuable discussions. This work was supported by the Centre National de la Recherche Scientifique and the Association de Recherches sur le Cancer (grant No. 9826) and Russian Foundation for the Basic Science (grants No.

97-04-48624 and 98-04-22055). Andrei V. Maksimenko was supported by the fellowship from the President of Russia.

## REFERENCES

1. Curcio, L.D.; Bouffard, D.Y.; Scanlon, K.J. *Pharmacol. Ther.*, **1997**, *74*, 317-332.
2. Wyngaarden, J.; Potts, J.; Cotter, F.; Martin R.R.; Mehta, V.; Agrawal, S.; Eckstein, F.; Levin, A.; Black, L.; Cole, R.; Crooke, S.; Kreig, A.; Diasio, R.; Gait, M.J. *Nature Biotech.*, **1997**, *15*, 519-524.
3. Agrawal, S. *Trends Biotech.*, **1996**, *14*, 376-387.
4. Wickstrom, E. *J. Biochem. Biophys. Methods*, **1986**, *13*, 97-102.
5. Eder, P.S.; Devine, R.J.; Dagle, J.M.; Walder, J.A. *Antisense Res. Dev.*, **1991**, *1*, 141-151.
6. Uhmalm, E.; Peyman, A. *Chem. Reviews*, **1990**, *90*, 544-584.
7. Stein, C.A.; Cohen, J.S. *Cancer Res.*, **1998**, *48*, 2659-2668.
8. Nielsen, P.E. *Ann. Rev. Biophys. Biomol. Struct.*, **1995**, *24*, 167-183.
9. Morvan, F.; Porumb, M.; Degols, G.; Lefebvre, I.; Pompon, A.; Sproat, B.S.; Rayner, B.; Malvy, C.; Lebleu, B.; Imbach, J.-L. *J. Med. Chem.*, **1993**, *36*, 280-283.
10. Stein, C.A. *Chemistry & Biology*, **1996**, *3*, 319-323.
11. Agrawal, S.; Zhao, Q.; Jiang, Z.; Oliver, C.; Giles, H.; Heath, J.; Serota, D. *Antisense & Nucl. Acid Drug Dev.*, **1997**, *7*, 575-584.
12. Branch, A.D. *TiBS*, **1998**, *23*, 45-50.
13. Jansen, B.; Wadl, H.; Inoue, S.A.; Trulzsch, B.; Selzer, E.; Duchene, M.; Fichler, H.; Wolf, K.; Pehamberger, H. *Antisense Res. Dev.*, **1995**, *5*, 271-277.
14. Henry, S.P.; Zuckerman, J.E.; Rojko, J.; Hall, W.S.; Harman, R.J.; Kitchen, D.; Crooke, S.T. *Anti-Cancer Drug Design*, **1997**, *12*, 1-4.
15. Khan, I.M.; Coulson, M. *Nucl. Acids Res.*, **1993**, *21*, 2957-2958.
16. Poddevin, B.; Meguenni, S.; Elias, I.; Vasseur, M.; Blumenfeld, M. *Antisense Res. Dev.*, **1994**, *4*, 147-154.
17. Yoshizawa, S.; Ueda, T.; Ishido, Y.; Miura, K-i.; Watanabe, K.; Hirao, I. *Nucl. Acids Res.*, **1994**, *22*, 2217-2221.
18. Tang, J.Y.; Tamsamani, J.; Agrawal, S. *Nucl. Acids Res.*, **1993**, *21*, 2729-2735.
19. Kuwasaki, T.; Hosono, K.; Takai, K.; Ushijima, K.; Nakashima, H.; Saito, T.; Yamamoto, N.; Takaku, H. *Biochem. Biophys. Res. Com.*, **1996**, *228*, 623-631.
20. Barker, R.H.; Metelev, V.; Coakley, A.; Zamecnik, P. *Exp. Parasitology*, **1998**, *88*, 51-59.
21. Ivanovskaya, M.G.; Gottikh, M.B.; Shabarova, Z.A. *Nucleos. Nucleot.*, **1987**, *5*, 913-934.
22. Petersheim, M.; Turner, D.H. *Biochem.*, **1983**, *22*, 256-263.
23. Bradford, M.M. *Anal. Biochem.*, **1976**, *72*, 248-254.
24. Hoke, G.D.; Draper, K.; Freier, S.M.; Gonzalez, C.; Driver, V.B.; Zounes, M.C.; Ecker, D.J. *Nucleic Acids Res.*, **1991**, *19*, 5743-5748.
25. Capaccioli, S.; Di Pasquale, G.; Mini, E.; Mazzei, T.; Quattrone, A. *Biochem. and Biophys. Res. Com.*, **1993**, *197*, 818-825.
26. Chavany, C.; Saison-Behmoaras, T.; Le Doan, T.; Puisieux, F.; Couvreur, P.; Helene, C. *Pharm. Res.*, **1994**, *11*, 1370-1378.
27. Delong, R.; Stephenson, K.; Loftus, T.; Fisher, M.; Alahari, S.; Nolting, A.; Juliano, R. L. *J. Pharm. Sci.*, **1997**, *86*, 762-764.
28. Morris, M. C.; Vidal, P.; Chaloin, L.; Heitz, F.; Divita, G. *Nucleic Acids Res.*, **1997**, *25*, 2730-2736.

29. Poxon, S. W.; Mitchell, P. M.; Liang, E.; Hughes J. A. *Drug Delivery*, **1996**, *3*, 255-261.
30. Schaw, J.-P.; Kent, K.; Bird, J.; Fishback, J.; Froechler, B. *Nucleic Acids Res.*, **1991**, *19*, 747-750.
31. Couch, R.J. *New Biologist*, **1990**, *2*, 771-777.
32. Kukowska-Latallo, J.F.; Bielinska, A.U.; Jonson, J.; Spindler, R.; Tomalia, D.A.; Baker, J.R. *Proc. Natl. Acad. Sci. USA*, **1996**, *93*, 4897-4902.
33. Bielinska, A.; Kukowska-Latallo, J.F.; Jonson, J.; Tomalia, D.A.; Baker, J.R. *Nucleic Acids Res.*, **1996**, *24*, 2176-2182.
34. Tang, M.X.; Redemann, C.T.; Szoka, F.C. *Bioconjugate Chem.*, **1996**, *7*, 703-714.

Received 1/15/99

Accepted 6/16/99